Journal of Materials and Environmental Science
ISSN : 2028-2508
e-ISSN : 2737-890X
CODEN : JMESCN

J. Mater. Environ. Sci., 2025, Volume 15, Issue 6, Page 1063-1079

http://www.jmaterenvironsci.com

Experimental study of the mechanical properties and shrinkage prediction model of concrete containing waste foundry sand

A. Akeb [1] *, S. Kherbache [1], A. Tahakourt [1], F. Bouziadi [2], B. Boulekbache [2]

[1] *Laboratory of construction engineering and architecture, University of Bejaia 06000, Algeria*

[2] *Laboratory of Materials Sciences and Environment, Hassiba Benbouali University of Chlef 02000, Algeria.*

**Corresponding author, Email address: akeb.ahlem@gmail.com*

***Received** 20 Sept 2024,*
***Revised** 16 May 2025,*
***Accepted** 18 May 2025*

Keywords:
- ✓ *Industrial waste;*
- ✓ *Concrete;*
- ✓ *Mechanical properties;*
- ✓ *Shrinkage;*
- ✓ *Model.*

***Citations:** Akeb A., Kherbache S., Tahakourt A., Bouziadi F., Boulekbache B. (2025) Experimental study of the mechanical properties and shrinkage prediction model of concrete containing waste foundry sand, J. Mater. Environ. Sci., 16(6), 1063-1079*

Abstract: The aim of this study is to develop a new, efficient, and inexpensive natural This paper is an experimental and numerical study of the possibility of producing concrete containing a by-product of the foundry industry, known as waste foundry sand (WFS), intending to protect the ecosystem and environmental assets and preserve natural resources. Several properties are investigated, such as the chemical and physical composition of WFS, workability, mechanical properties and total shrinkage of different concretes. The concrete mixtures are manufactured by replacing natural sand with WFS at weight ratios of 10%, 20%, and 30%. The results indicated that the workability is reduced with rising WFS. However, an increase in the mechanical properties is observed up to 10% of WFS compared to the control concrete (CC), beyond this ratio, a decrease is noted. A decrease in the shrinkage at 180 days is found for the concrete with 10% of WFS compared to the CC but it increases with 20% and 30% substitution. Furthermore, a modified ACI-209 model is developed to predict the total shrinkage. This model included the percentage replacement of WFS. The modified model demonstrates a low value of residual error and an elevated coefficient of determination value, indicating its efficiency to predict the total shrinkage

1. Introduction

Waste foundry sand is the by-product of the ferrous and nonferrous metal casting industries. The waste generated by ferrous and nonferrous metal casting sectors is called waste foundry sand. It is comprised of high grade silica sand combined with binding agents (Thiruvenkitam, Pandian *et al*. 2020). Once the molten metal is introduced into the mould, the binders keep the sand together and keep it in form and help to maintain the shape of the sand during the pouring of molten metal into the mold.

There are various types of WFS depending on the binders, like green sand bounded with clay. It is made of 84–94% silica sand, 3–11% bentonite used as a binding agent and 3–9% of the carbonaceous substance added to enhance the final surface of the casting; or sand bonded chemically, it comprises between 92–98% of silica sand and 1–4% of the chemical binder. Generally, WFS is recycled and reused until its properties degrade to the point that it can no longer be utilized, at which point it is thrown from the foundry. This abandoned WFS became an environmental problem. Around one tonne of WFS is consumed for each tonne of steel or iron casting produced (Mavroulidou and Lawrence 2019).

Current studies report that the USA generates 6 to 10 million tonnes of WFS, of which only 15% is recycled and the rest is landfilled (Monosi, Tittarelli et al. 2013; Torres, Bartlett *et al*. 2017). In the UK, about 460 foundries produce copper, aluminium and iron castings, generating over one million tons of WFS every year (Khatib, Herki *et al*. 2013).

In Algeria, there are several foundry companies that have been manufacturing and marketing foundry products for more than 50 years, generating approximately 18,000 tons of cast iron and 5,500 tons of steel each year, as well as mechanical machining and industrial sheet metal work. The stock of WFS near the production units represents a threat to the environment, and this indicates the importance of the waste recovery. Therefore, the need to conduct studies and to think about effective solutions for its valorisation (Belmahi, Mohamed *et al*. 2021).

Waste foundry sand has been used in several ways in civil engineering, such as high way embankment construction (Ham, Boyle *et al*. 1986; Mast and Fox 1998; Kleven, Edil *et al.* 2000), *ground improvement* (Vipulanandan, Weng *et al*. 2000), hydraulic barrier or liner (Goodhue, Edil *et al*. 2001; Abichou., Edil. *et al*. 2004). Some studies reported leachability levels below regulated water's quality limits, also WFS has been employed with care in geotechnical and roadway applications because of fears of hazardous substance leaching (FIRST 2004). Using a waste aggregate in concrete reduces the need of non-renewable mineral-aggregate sources. However, before using WFS in concrete, it is important to consider how its grading, binders residues and surface properties may affect its suitability; due to because WFS being very fine, so it can't be used as a total sand substitution (FIRST 2004). Its fineness modulus is from 0.9 to 1.7, while natural sand has the range of 2.3 to 3.1 (Bhardwaj and Kumar 2017).

Contradictory results have been emerged concerning the impact of WFS on the mechanical properties of the concrete. Some researchers have found a significant improvement in the compressive strength owing to the replacement of natural sand with WFS, until a point when the strength started to decrease (Singh and Siddique 2012; Siddique, Singh *et al*. 2015; Gurumoorthy and Arunachalam 2016; Manoharan, Laksmanan *et al*. 2018; Mavroulidou and Lawrence 2019; Thiruvenkitam, Pandian *et al*. 2020). However, other studies have found that the strength of concrete diminishes when the percentage of WFS rises (Khatib, Baig *et al*. 2010; Basar and Aksoy 2012; Monosi, Tittarelli *et al.* 2013; Parashar, Aggarwal *et al.* 2020).

Thiruvenkitam et al. (Thiruvenkitam, Pandian *et al.* 2020) have measured the compressive strength of concrete with different percentages of chemically bonded foundry sand (5, 10, 15, 20 and 25%). The findings indicated an increase in strength with increasing WFS replacement up to 20%, after which it started to decrease. This is due to the cementitious substance adhering to the WFS particles' smaller surfaces. Once the replacement percentage exceeded 15%, the resistance steadily decreased. Similar outputs were observed for split tensile strength, flexural strength, and modulus of elasticity.

Kaur et al. (Kaur, Siddique *et al.* 2012) observed that the control mix had a compressive strength of 33 MPa at 28 days, whereas concrete with 10%, 15%, and 20% WFS (untreated one) exhibited respective compressive strengths of 33, 29 MPa, and 27 MPa. WFS (fungal treated) had a compressive strength of 36, 32, 32 MPa in concrete with 10%, 15%, and 20% WFS, respectively. Mavroulidou and Lawrence (Mavroulidou and Lawrence 2019) indicated that the physical characteristics of WFS are suitable for usage in the matrix. They reported that the increase in strength is assigned to the filler effect of finer, uniform and rounder WFS, which reduces the pores ratio in the concrete.

Shrinkage is another property that should be taken into consideration when producing concrete elements for structural purposes, since greater shrinkage means a greater extent of cracking. This can allow harmful agents to enter concrete, which might result in the corrosion of structural concrete's steel reinforcements, and could compromise the safety of the structure. Various parameters affect the shrinkage rate including the aggregates, the curing period, water/binder ratio, ambient factors, mineral admixtures, The amount, quality, and grading of aggregates significantly influence concrete shrinkage (Zhu, Wei *et al.* 2016). Aggregates may shrink, and this might have a big impact on the shrinkage (Fujiwara 2008). Few studies have examined the shrinkage of concrete containing WFS. Research conducted by Khatib et al. (Khatib, Baig *et al.* 2010), Jose and Hossiney (Jose and Hossiney 2016) claim that the addition of WFS increased the drying shrinkage.

Mushtaq et al. (Mushtaq, Siddique *et al.* 2021) have reported that the shrinkage rised when WFS increased. The increase in shrinkage was attributed to the higher compressibility of the WFS in comparison to the natural sand. However, limit researches have been carried on the influence of the WFS on the total shrinkage of concrete.

Different numerical models have been created to predict the concrete shrinkage like ACI-209 Model (ACI-209 2R-08 2008), Bazant B3 Model (Bazant and Murphy 1995), CEB MC90 Model (Hooton 1993), Mushtaq et al. (Mushtaq, Siddique *et al.* 2021) investigated the shrinkage of concrete with WFS using the ACI-209 model. Furthermore, few models are available in the literature to predict the total shrinkage of concretes made with WFS as an alternative to the ordinary sand.

The objective of this study is to assess the influence of the use of WFS as fine aggregate on the workability, the mechanical properties and the total shrinkage of concrete. The mixes incorporating WFS are made by replacing 10%, 20%, and 30% of natural sand with WFS. In addition, a modified ACI-209 model based on experimental findings is developed to predict the total shrinkage of concretes containing different percentages of WFS as fine aggregate.

2. Materials and Methodology

2.1 Materials used

2.1.1 Cement

The cement used in all mixtures is a CEM II/A-L 42.5 N based on the European standard EN 197-1 *(BS 197-1 2011)*, with a density of 3.1 g/cm3 and a specific surface area of 3866 cm2/g. **Table 1** shows the composition of this cement.

Table 1. Chemical and mineralogical composition of cement

Chemical composition	
SiO2	20.69
Al2O3	4.73
Fe2O3	3.92
CaO	60.35
MgO	1.31
SO3	2.02
K2O	0.32
Na2O	0.13
Mineralogical composition	
C3S	55.46
C2S	18.85
C3A	8.56
C4AF	12.43

2.1.2 Foundry sand

The WFS used is a by-product from the foundry industry BCR in Setif (Algeria). The industry uses it to make moulds and cores. Each mixture is composed of: 40 kg of siliceous sand, 0.980 kg of resin and 0.280 kg of catalyst. After use in industry, it was rejected and considered as foundry waste **(Figure 1(a)).** To use it in concrete, it was cleared of lumps or dust then crushed **(Figure 1(b)).** The WFS showed a lesser water absorption than natural sand in spite of its finer size (**Table 2**), which can be due to the water-repelling binder remnants (Mavroulidou and Lawrence 2019). According to **Figure 2**, WFS was very uniform unlike the well-graded natural sand. The different properties of all aggregates are given in **Table 2.**

(a) Cores of WFS (b) WFS crushed in laboratory (c) Morphology of WFS (SEM)

Figure 1. Photography of WFS

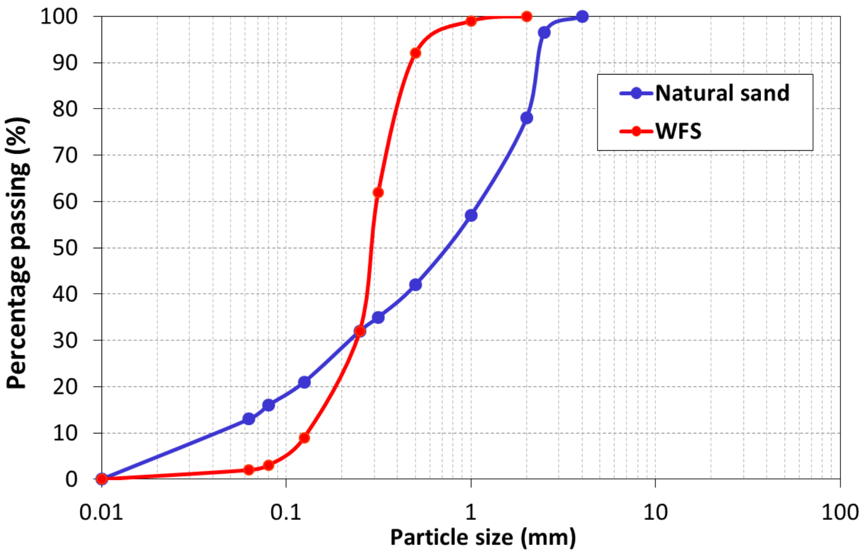

Figure 2. Particle size distributions.

2.1.3 Aggregates

Coarse aggregates from the quarry of ENOF in Setif (Algeria) were used in this study. Natural sand with maximum size 4 mm, and crushed stone aggregates are used for the manufacture of concretes. In order to define the chemical composition and the particle morphology of the WFS, X-ray diffraction (XRD) analysis, Scanning Electron Microscopy (SEM) and sight energy-dispersed spectrum (EDS) were used. According to the SEM analysis, WFS particles are rounded or sub-angular in shape (Fig. 1(c)), The XRD analysis confirmed that SiO2 is the main constituent in the WFS (Quartz was given credit for all major peaks (Fig. 3(a)). The EDS results showed a higher Si content (higher peaks) and lower O content, which was indicative of organic binder remnants (Fig. 3(b)). Small peaks of Al, Fe, and Mg are also observed. Mavroulidou and Lawrence (Mavroulidou and Lawrence 2019) have also found that Si was the main element present in all sites.

Table 2. Properties of aggregates

	Natural sand	WFS	Coarse aggregate
Fineness modulus	**2.69**	**1.69**	**/**
Sand equivalent	**71**	**82**	**/**
Methylene blue value	**1**	**0.35**	**/**
Bulk density (g/cm3)	**1.66**	**1.39**	**1.50**
Specific gravity (g/cm3)	**2.73**	**2.58**	**2.79**
Water absorption (%)	**0.83**	**0.45**	**0.9**
Los-Angeles coefficient (%)	**/**	**/**	**20**

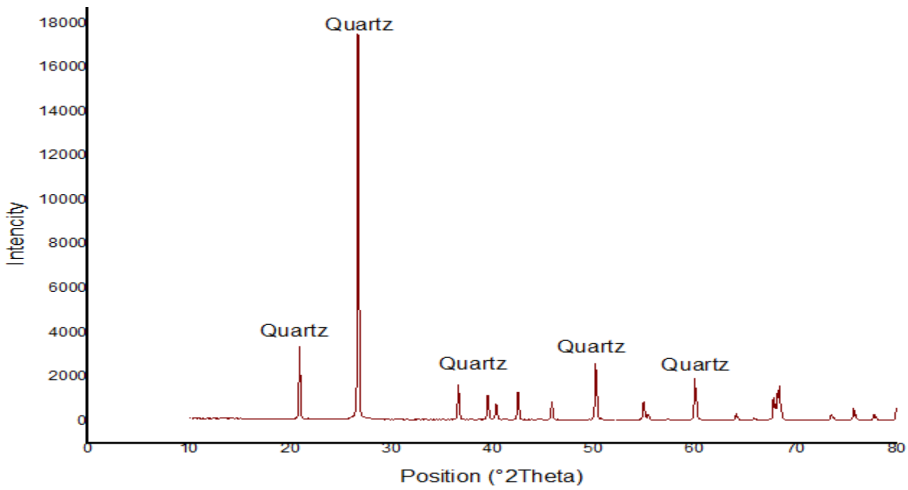

Figure 3a. X-ray diffraction of WFS

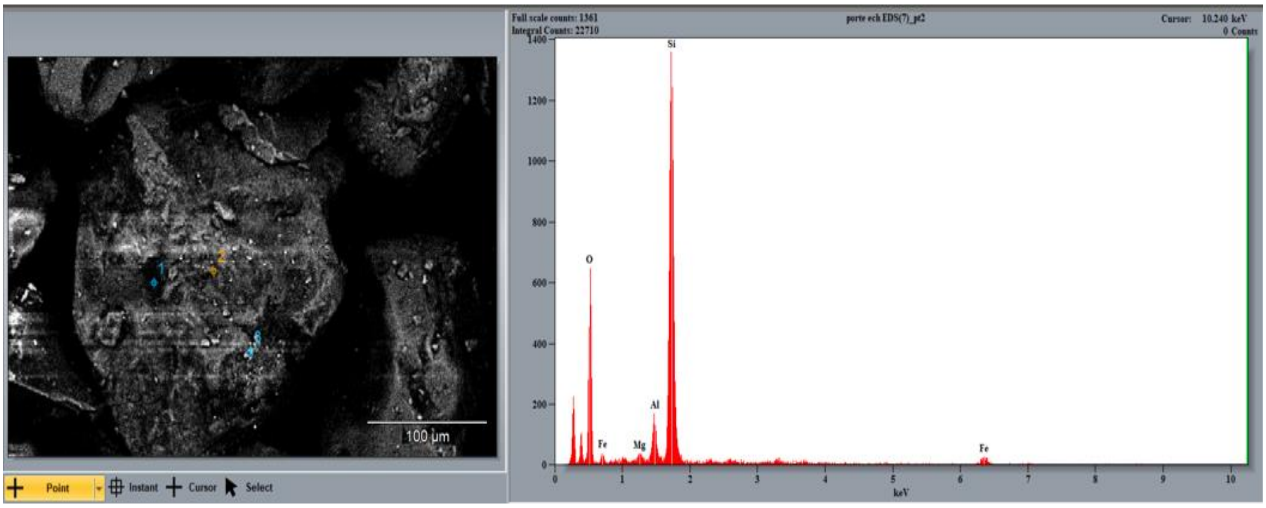

Figure 3b. Chemical composition of WFS

2.1.3 Superplasticizer

A water reducer superplasticizer of last generation (CHRYSO-Fluid Optima 208A) was used to maintain workability and ensure concrete cohesion. It has a dosage of 0.7% by weight of the cement and meets the requirements of the NF EN 934-2 standard (NF EN 934-2 2012).

2.2 Concrete mix

Four concrete mixtures were manufactured. The first one was the control concrete (CC), in the three additional concrete mixtures (WFSC10, WFSC20 and WFSC30), the natural sand was replaced by 10%, 20%, and 30% of WFS by weight, respectively. The water-cement ratio (W/C) was kept at 0.5 of all the mixes. After mixing the dry constituents, the water was added: half immediately before the mixer's rotation began, and half was added along with the superplasticizer during the mixing process. Three distinct layers of compacted specimens were cast in moulds and vibrated into place. Details of the mixtures and temperature are presented in **Table 3.** After mixing, the moulds were stored at 20 °C and 90% moisture. After one day, specimens were demoulded, labelled, and stored in a water tray at room temperature (20 °C ±2 °C), until the testing age.

Table 3. Mix design proportions (kg/m3).

	CC	**WFSC10**	**WFSC20**	**WFSC30**
Cement	350	350	350	350
Natural sand	831	748	665	582
WFS (%)	0	10	20	30
WFS	0	83	166	249
Coarse aggregate	1006	1006	1006	1006
Water	175	175	175	175
W/C	0.5	0.5	0.5	0.5
Superplasticizer	2.45	2.45	2.45	2.45
Air temperature (°C)	24	25	24	23
Concrete temperature (°C)	27	28	27	28

2.2.1 Mechanical properties

For each mix, three cubic samples (150 mm) were prepared to measure the compressive strength at 7, 28 and 90 days based on EN 12390-3 (EN 12390-3 2003). Three prismatic specimens 70×70×280 mm were produced for each mixture to evaluate the flexural strength at 28 days as per as EN 12390-5 (EN 12390-5 2001). Three cylinders 160×320 mm were also used for the evaluation of the modulus of elasticity using an extensometer conforming to ASTM C469 (ASTM C469 2014).

2.2.2 Total shrinkage

Prismatic moulds of 100×100×400 mm were made for the realization of the test, and a pair of copper pads distanced 100 mm apart was placed on the specimens. After making, the moulds were coated with nylon to avoid evaporation at early age. After demoulding, a layer of asphalt was applied to both ends to preserve the edges and prevent water contact for the proper conduct of the test. The samples are maintained vertically in a steam oven at 20 °C with relative humidity of 50%.

To measure the shrinkage, a digital comparator with a precision of 1 µm was used as illustrated in **Figure 4.** Measurements are taken in four time periods: the initial timeline one per hour for one week. The second timeline occurs twice daily for two weeks, the third timeline once daily for one week and once monthly for five months (Bouziadi, Boulekbache *et al.* 2016).

Figure 4. Shrinkage test

3. Results and Discussion

3.1 Workability

The results of the slump test determined as per (NF EN 12350-2 2019), are shown in Figure. 5. The workability of concrete decreases when WFS increases in constant W/C ratio. The loss of workability is due to the higher surface area of WFS compared to natural sand. Indeed, the particles are more uniform in size and finer, requiring more water to reach the necessary workability. This result is confirmed by Manoharam et al. (Manoharan, Laksmanan *et al*. 2018) and Prabhu et al. (Prabhu, Hyun et al. 2014).

3.2 Compressive strength

Figure 6 shows the compressive strength of different concretes at 7, 28, and 90 days. The findings indicate that the compressive strength of all tested mixtures increases with age and is influenced by the amount of WFS. After 28 days, CC had a strength of 52.8 MPa, whereas WFSC10, WFSC20, and WFSC30 had strengths of 72.3, 64.3 and 48.5 MPa, respectively.

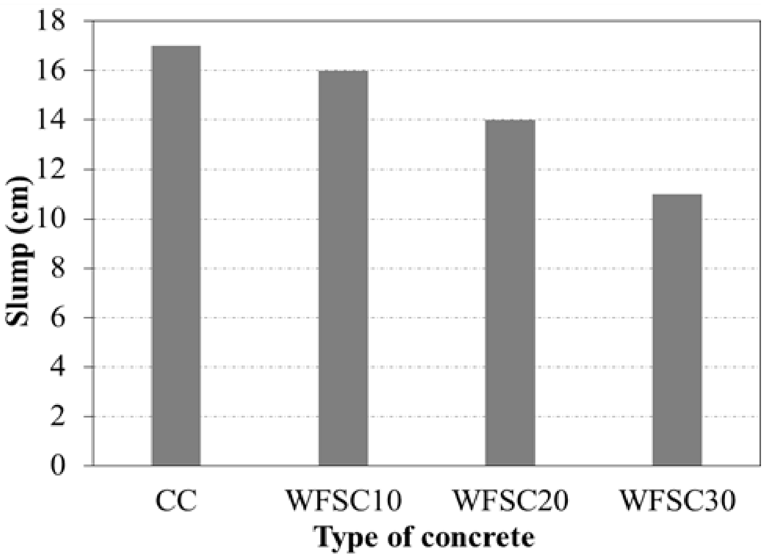

Figure 5. Slump test

WFSC10 showed the optimal replacement level of WFS where the increase of strength achieved 36.9% compared to the CC, while it was 21.8% for WFSC20. It can indicate that the particle-size distribution of WFSC10 has better adherence than the other mixtures (Guney, Sari *et al*. 2010), giving a denser matrix. Additionally, the silica present in the WFS (Siddique, De Schutter *et al*. 2009) and some filler effect of the uniform and finer WFS may reduce the void ratios (Mavroulidou and Lawrence 2019). The reduction in strength for WFSC30 was 8.14% compared to the CC. This is because fine particles have more surface area, which reduces the amount of water cement gel in the matrix (Siddique, Singh *et al*. 2015). At 90 days, concrete with 20% WFS exhibited almost the same strength as the CC, whereas WFSC30 shows slight values than that of the CC. Based on these results, WFS can successfully replace fine aggregate up to 20% by weight.

Parashar et al. (Parashar, Aggarwal *et al*. 2020) also achieved the same results. Additionally, Siddique et al. (Siddique, Singh et al. 2015) also noted a rise in compression strength up to 15% of WFS, before diminishing after this point. Thiruvenkitam et al. (Thiruvenkitam, Pandian *et al*. 2020) and Manoharan et al. (Manoharan, Laksmanan *et al*. 2018) added that the increase can be observed up to 20% of WFS.

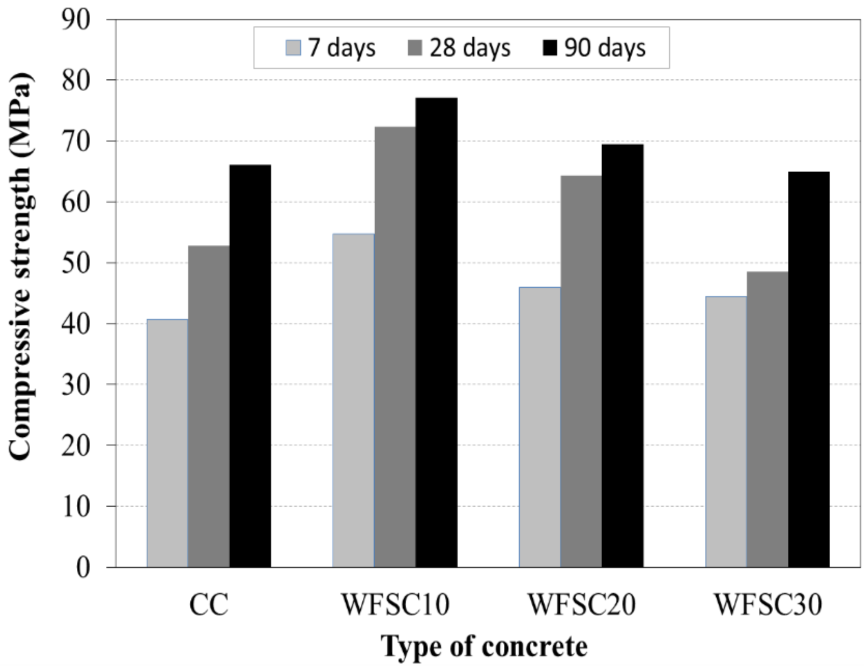

Figure 6. Compressive strength results**.**

3.3 Flexural strength

Figure 7 displays the results of the flexural strength test of 28 days cured concrete with various WFS replacement. The flexural strength of the CC was found 6.4 MPa and it increased by 12.9% for the mix WFSC10, then, it decreased by 9.4% and 21.9% for the WFSC20 and WFSC30, respectively. According to Thiruvenkitam et al. (Thiruvenkitam, Pandian *et al*. 2020), the WFS had a favourable effect on the flexural strength of concrete up to 15% replacement, but with further use, a negative effect was observed. Manoharan et al. (Manoharan, Laksmanan *et al*. 2018) and Prabhu et al. (Prabhu, Hyun *et al*. 2014) reported an initial increase up to 20% WFS replacement due to the filler effect, then the reduction in strength was caused by an excess of fine particles that were not used in the concrete.

3.4 Modulus of elasticity

The modulus of elasticity was measured at 28 day. The influence of the WFS on concrete is shown in **Figure 8**. It is obvious that with the addition of WFS up to 10% replacement, the modulus of elasticity increased with 10.1% compared to CC, then a reduction was observed for the mixes WFSC20 and WFSC30 to achieve 4.3% and 7.5%, respectively. This could be due to the packing behaviour between the particles. Beyond 10% replacement, no more fine particles required to fill the voids between the particles (Siddique, Singh *et al*. 2015). Similar results were reported by Mavroulidou and Lawrence (Mavroulidou and Lawrence 2019). Siddique et al. (Siddique, Singh *et al.* 2015) and Thiruvenkitam et al. (Thiruvenkitam, Pandian *et al.* 2020) also concluded that the modulus of elasticity increased up to 15% WFS content.

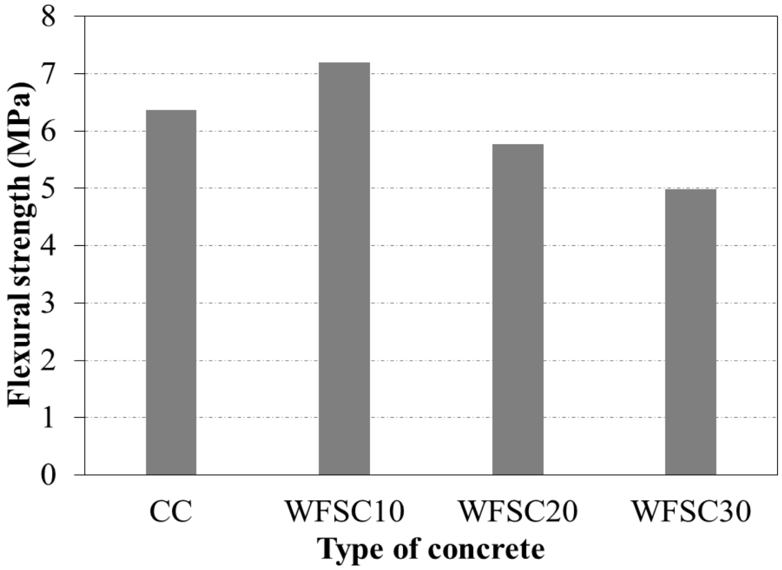

Figure 7. Flexural strength results at 28 days.

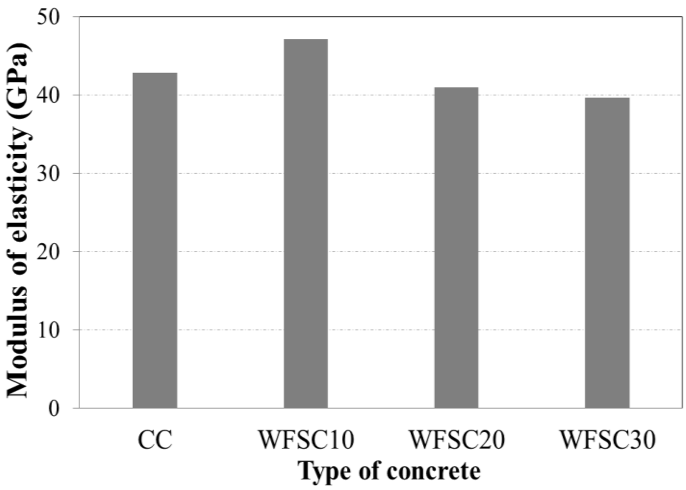

Figure 8. Modulus of elasticity results at 28 days

3.5 Total shrinkage

The total shrinkage values for all the mixtures as a function of time, from 1 to 180 days, are shown in **Figure 9**. The shrinkage rate of all mixes is faster in the early drying stages than it is at later ages. The shrinkage values of concrete containing WFS were discovered to be very similar to CC values at an early age. It was found that the total shrinkage of WFSC10 was around 11.5%, 6.2%, and 2.6% lower than CC, at 28, 90 and 180 days, respectively. For the WFSC20 mix, the total shrinkage decreased by 6.8% at 28 days, whereas it increased by 2.6% at 180 days. Finally, for WFSC30, the total shrinkage amounted to 8.1%, 4.8% and 5.1% at 28, 90 and 180 days, respectively compared to CC.

According to Mushtaq et al. (Mushtaq, Siddique *et al.* 2021) the shrinkage rose as the amount of WFS rose. Khatib et al. (Khatib, Baig *et al.* 2010) found that the addition of WFS increased the drying shrinkage, and they observed that for 100% sand replacement with WFS, the shrinkage at 56 days was twice as much as the CC. The higher compressibility of WFS compared to ordinary sand may be the cause of the increase in the shrinkage (Mushtaq, Siddique *et al.* 2021). As it was found in the WFSC10 compared to CC, the compactness lost can be restored due to the densification of the microstructure, and concrete exhibits lesser shrinkage, when if the WFS used is sufficient to fill all the voids.

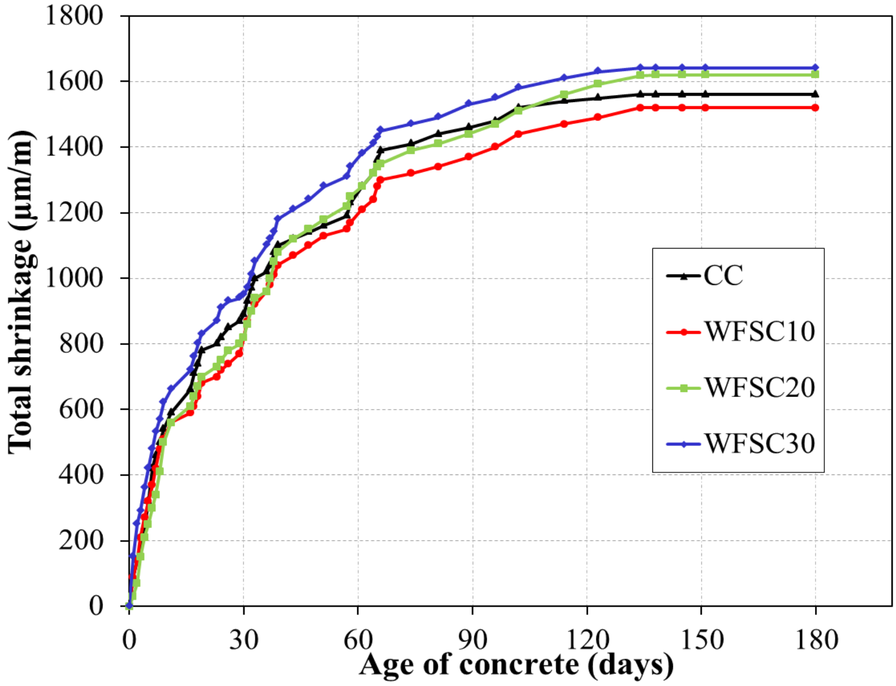

Figure 9. Influence of WFS on the total shrinkage.

3.6 Micro-structural analyses

3.6.1. X-ray diffraction (XRD)

The concrete mixtures were examined using XRD method at 365 days. X-ray diffraction patterns of the control concrete and concrete containing WFS are illustrated in **Figures 10(a-d).** The findings show the presence of quartz, calcite, CSH, and portlandite in all the mixtures. The intensity of SiO2 at 31°2θ reached 4200, 4500, 4450 and 4500 for CC, WFSC10, WFSC20 and WFSC30, respectively. The determination of CSH could not be performed because it has an amorphous structure and XRD analysis is performed for single crystal and polycrystalline. According to Aggarwal and Siddique (Aggarwal and Siddique 2014), the XRD pattern observed in mix with 10% of WFS was similar to CC. They concluded that the main component consisted of highly crystalline quartz compounds, as shown in the graphs obtained at various 2θ values.

3.6.1. Scanning electron microscope (SEM) analysis

In order to examine the crystal morphology and surface texture, SEM images were used. The bright and dark matter in the pictures represent the C-S-H gel/ paste and inert aggregates, respectively. The distinction between the various particles of inert aggregates was made by identifying carried out as the medium dark particles being thought of as WFS particles and the dark particles referred to coarse aggregates (Aggarwal and Siddique 2014). Since these medium-dark particles are observed in almost all samples containing WFS particles, with the exception of the CC mixture, these assumptions can be justified. The micrograph of CC is represented in **Figure 11(a),** the C-S-H and pores can be easily distincted, the C–S–H gel is distributed over the entire micrograph.

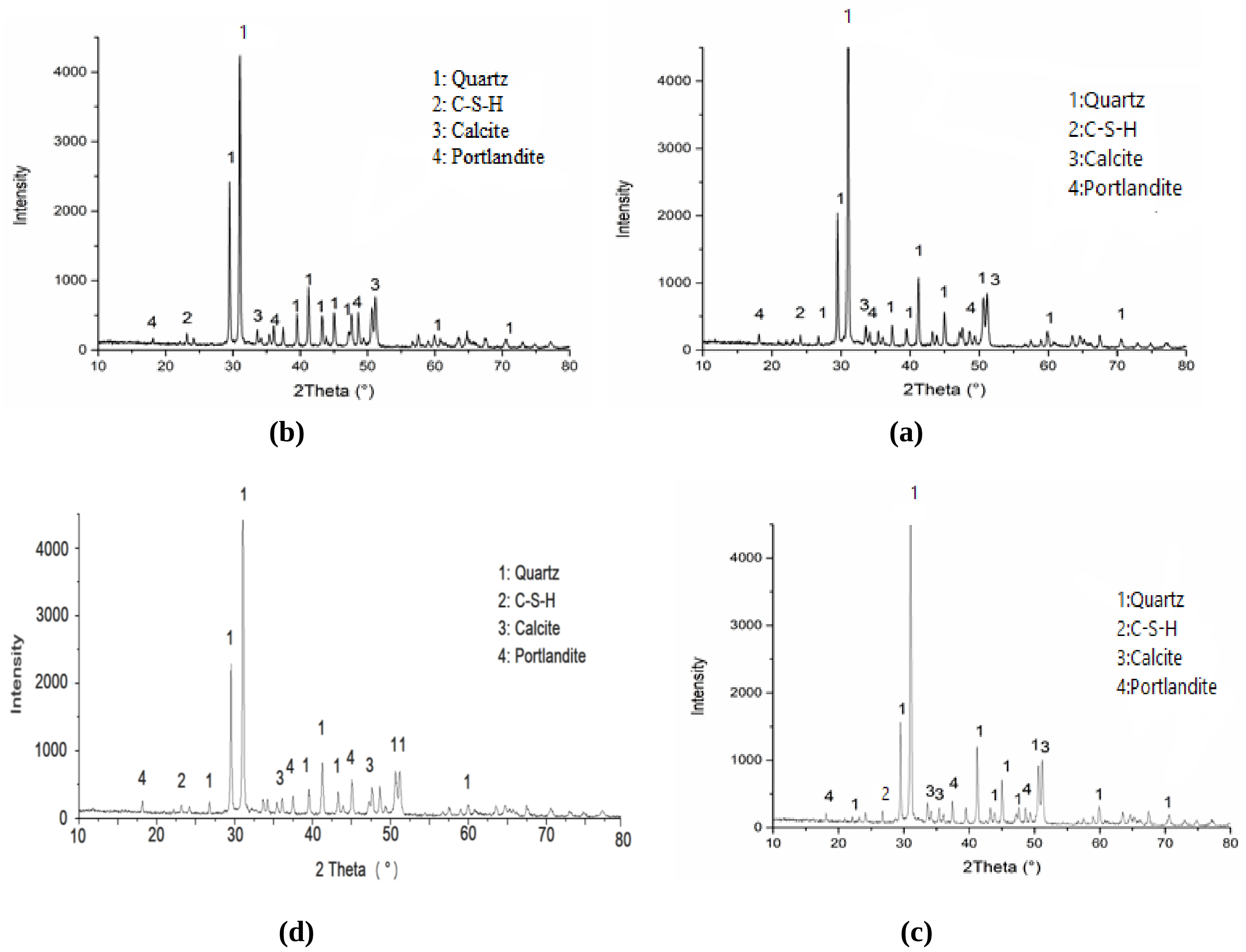

Figure 10. X-ray diffraction patterns of different mixture

(a) CC (b) WFSC10 (c) WFSC20 (d) WFSC30

Figure 11(b) shows the micrograph of WFSC10. As it can be seen, the number of voids in the mix has significantly decreased, which was confirmed by an increase in strength. The image also indicates a comparative densification of the matrix (high amount of C–S–H gel). The SEM image of WFSC20 shows that the mixture has less C–S–H gel than WFSC10 and more voids, as shown in **Figure 11(c).** The increase in WFS causes a noticeable difference on the surface of WFSC30, as it is shown in **Figure 11(d),** which was confirmed by a reduction in strength due to the presence of an excess of fine particles, more porosity, and insoluble residues.

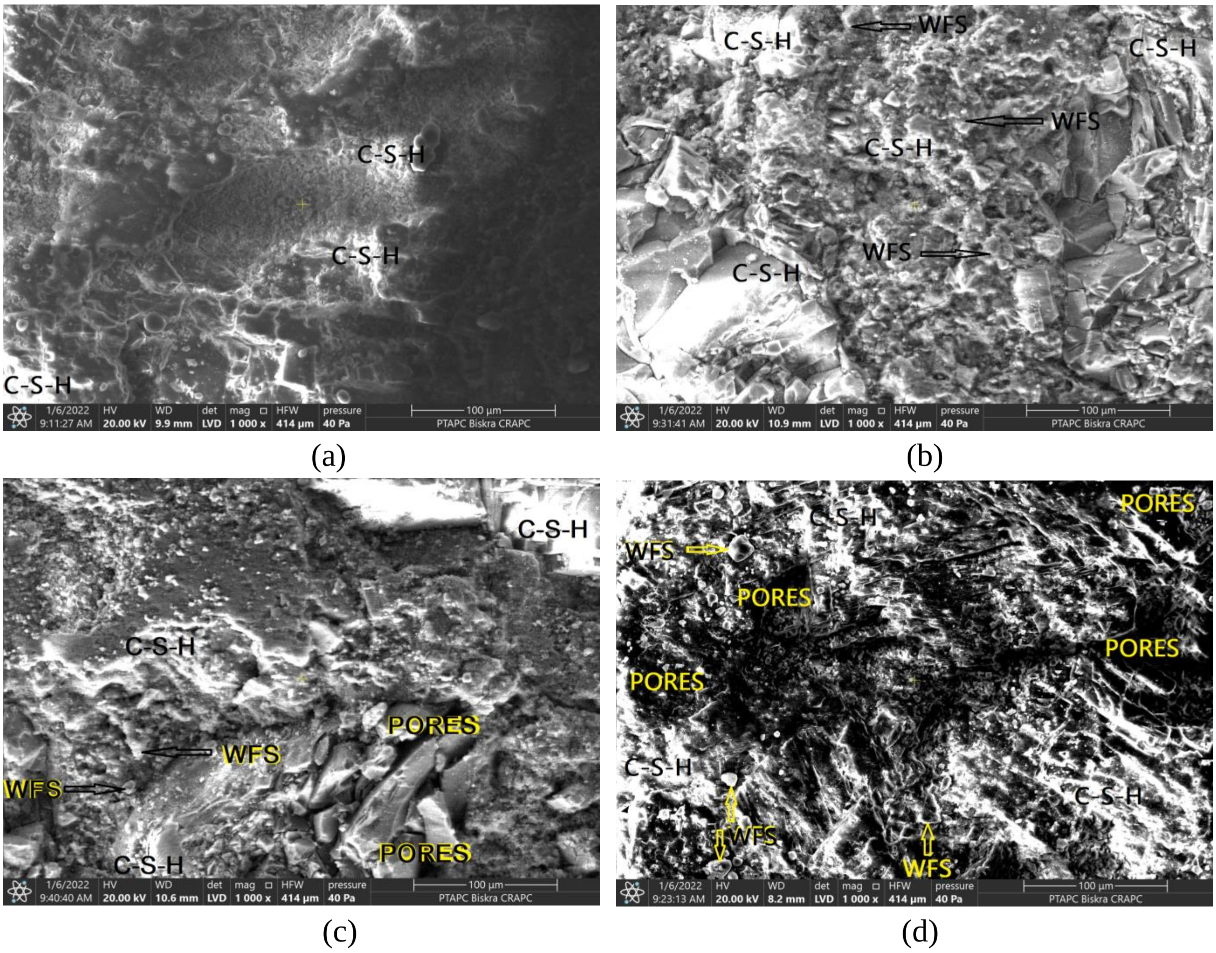

Figure 11. SEM photographs.

(a) CC (b) WFSC10. (c) WFSC20. (d) WFSC30.

4. Numerical investigation

4.1. Prediction model of the shrinkage of concrete containing WFS

Several models were proposed to predict the shrinkage of concrete. The ACI-209 model is the most popular one due to its simplicity in application, requiring lesser input variables (Siddique, De Schutter *et al*. 2009).

4.2. ACI-209 model

ACI-209R-92 *(Aggarwal and Siddique 2014)* proposes the following general hyperbolic function (**Eqn. 1**) for predicting the shrinkage of concrete at time t:

$$\varepsilon = \frac{t}{f+t}\varepsilon_u \qquad \textbf{Eqn. 1}$$

where ε is the shrinkage at time t, εu is the ultimate shrinkage of concrete and f is the constant determined by linear regression fitting analysis using the ordinary least squares method of the data obtained experimentally.

However, the ACI-209 model needs the incorporation of a parameter based upon the percentage of WFS replacement. Thus, in this study, the ACI-209 model has been modified to predict the shrinkage of concrete considering the percentage replacement of WFS.

4.3. Modified ACI-209 model

The aim of this section is to modify the ACI-209 model to predict the total shrinkage of concrete containing WFS using a linear regression fitting analysis of the experimental data. **Figure 12** shows the fitting of the experimental results of total shrinkage of concrete containing WFS using the linear regression fitting analysis with the ordinary least squares method. The objective is to present a model that can predict the shrinkage at any time. The hyperbolic function chosen to predict the total shrinkage of concrete containing WFS based on the ACI-209 model is shown as follows **Eqn. 2:**

$$\varepsilon = \frac{a\,t}{b+t} \qquad \textbf{Eqn. 2}$$

where a and b are constants determined by linear regression fitting analysis with the ordinary least squares.

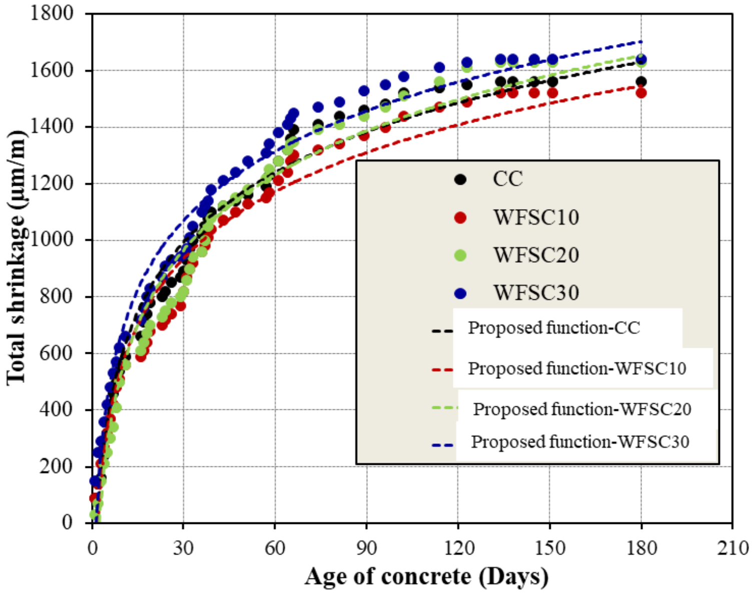

Figure 12. Fitting of the experimental results of total shrinkage of concrete containing WFS.

The values of constants a, b and coefficient of determination (R^2) for each concrete are summarized in **Table 4**.

Table 4. Value of coefficients a, b and R^2.

	a	**b**	**R^2**
CC	1877.89	28.27	0.99
WFSC10	1900	32.50	0.99
WFSC20	2069.19	38.54	0.99
WFSC30	2145	45	0.99

Constants a and b are quantified on the basis of the percentage replacement of WFS. As shown in **Figure 13,** the experimental shrinkage constants a and b are plotted against percentage replacement of WFS, and linear equation fits are performed to achieve the objective of this study. According to the values of R2, all linear function curves fit the experimental data of constants a and b well. **Eqns 3** and **Eqns 4** show the expressions obtained for these constants:

$a = 970.5\, W + 1852.4$ ***Eqn. 3***

$b = 56.23\, W + 27.64$ **Eqn. 4**

where W is the percentage replacement of WFS.

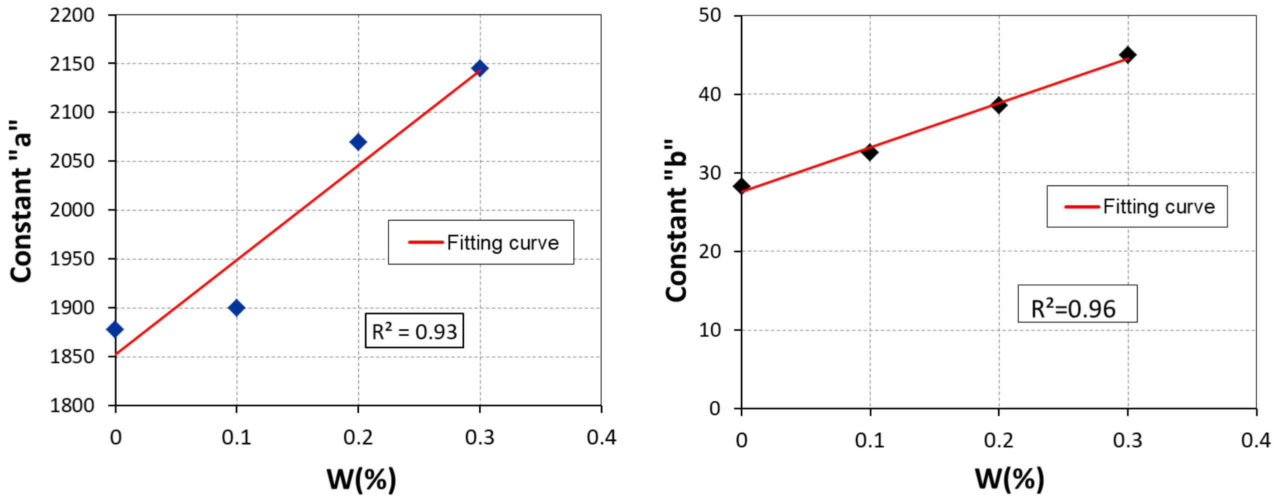

Figure. 13. Determination of constants a and b.

4.4. Accuracy of the modified ACI-209 model

The modified ACI-209 model described above is validated against the realized experimental results. The accuracy of the modified ACI-209 model can further be confirmed by performing the percentage residual error analysis. The percentage residual error can be calculated as follow in **Eqn. 5**:

$$Residual\ error\ (\%) = \frac{Predicted\ shrinkage - Experimental\ shrinkage}{Experimental\ shrinkage} \times 100 \qquad \textbf{Eqn. 5}$$

Table 5 shows the percentage residual errors for different concrete mixtures used in this study. Hence, it can be concluded that the modified ACI-209 model given in **Eqns 2** is reasonably accurate and effective in predicting the shrinkage of concrete containing WFS. However, it should be noted here that the modified ACI-209 model is developed for percentage of WFS lying between 0 and 30%.

Table 5. Residual error of predicted shrinkage values for different concrete.

Age (days)	**Residual error (%)**			
	CC	**WFSC10**	**WFSC20**	**WFSC30**
3	7.85	8.69	8.85	9.56
7	7.65	7.85	6	8.56
28	6.98	-6.42	-4.58	5.87
90	-5.32	4.95	4.05	-4.63
180	2.58	-3.56	-3.87	-6.45

Further, a comparison of experimental shrinkage values with those obtained numerically for all data points is shown in **Figure 14**. It can be seen that the predicted shrinkage values do not differ much from the experimentally ones. The high R2 value of 0.96 indicates that the modified ACI-209 model can accurately predict the total shrinkage of concrete containing different replacements of WFS.

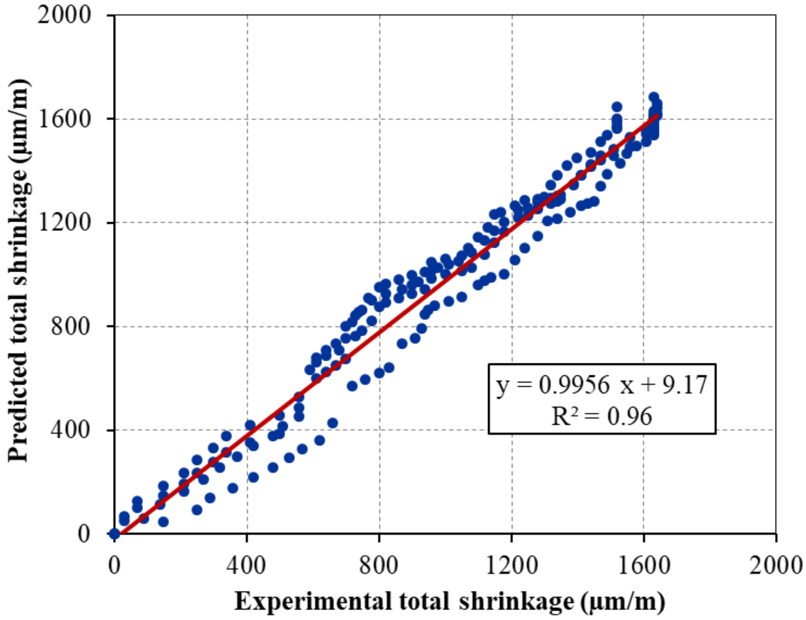

Figure 14. Experimental total shrinkage versus predicted total shrinkage for all data points.

Conclusion

In the current study, the use of WFS as a partial replacement of fine aggregate in concrete was investigated. The following conclusions can be drawn:

1. The use of WFS lead to decrease the workability of concrete, that can be due to the surface area of the WFS being higher than the natural sand.
2. Compressive, flexural strengths and the Young's modulus increased for 10% of WFS, and decreased beyond this substitution. Therefore, if the amount of WFS content utilized is just enough to fill the void, the lost strength can be restored due to the microstructure's densification,
3. The shrinkage of concrete increasesd with a rise in the addition of WFS after decreasesd for the WFSC10 mix. The shrinkage values are considerably higher at early ages.
4. A modified ACI-209 model is developed for prediction of total shrinkage of concrete containing WFS as fine aggregate taking into account the percentage replacement of WFS. This model gave a low value of residual error and a high value of the coefficient of determination, indicating the effectiveness to predict the total shrinkage of concrete containing of WFS as fine aggregate lying between 0 and 30%.

The co-conversion cost, high biochar yield and no electrical power requirement. The study has been able to successfully achieve the co-conversion of biomass and plastics (as typologies of MSW major components valuable products with a twin goal of waste management and product development.

Acknowledgement. The authors are pleased to acknowledge the support of the Ministry of Higher Education and Scientific Research of Algeria (MESRS).
Disclosure statement: *Conflict of Interest:* The authors declare that there are no conflicts of interest.
Compliance with Ethical Standards: This article does not contain any studies involving human or animal subjects.

References

Abichou. T., T. B. Edil., et al. (2004). "Beneficial use of foundry by-products in highway construction." *Geotechnical Engineering for transportation projects* 126, 715e722.

ACI-209 2R-08 (2008). Guide for modeling and calculating shrinkage and creep in hardened concrete: *American Concrete Institute*.

Aggarwal Y. and R. Siddique (2014). "Microstructure and properties of concrete using bottom ash and waste foundry sand as partial replacement of fine aggregates." *Construction and building materials* 54, 210-223.

ASTM C469 (2014). Standard Test Method for Static Modulus of Elasticity and Poisson's Ratio of Concrete in Compression. *ASTM International, West Conshohocken, PA* .

Basar H. M. and N. D. Aksoy (2012). "The effect of waste foundry sand (WFS) as partial replacement of sand on the mechanical, leaching and micro-structural characteristics of ready-mixed concrete." *Construction and Building Materials* 35, 508-515.

Bazant Z. P. and W. Murphy (1995). "Creep and shrinkage prediction model for analysis and design of concrete structures-model B3." *Matériaux et constructions* 28(180), 357-365.

Belmahi S., Z. Mohamed, et al. (2021). "Valuation of foundry sand in the construction sector." *Lebanese Science Journal* 22(1), 112.

Bhardwaj B. and P. Kumar (2017). "Waste foundry sand in concrete: A review." *Construction and Building Materials* 156, 661-674.

Bouziadi F., B. Boulekbache, et al. (2016). "The effects of fibres on the shrinkage of high-strength concrete under various curing temperatures." *Construction and building materials* 114, 40-48.

BS 197-1 (2011). "Cement–Part 1: Composition, specifications and conformity criteria for common cements." *London: European Committee For Standardisation.*

EN 12390-3 (2003). Part 3: Compressive Strength of Test Specimens, AFNOR.

EN 12390-5 (2001). Part 5: Flexural Strength of Test Specimens, AFNOR.

FIRST, F.-I. (2004). Foundry sand facts for civil engineers, Report No. FHWA-IF-04-004, Washington DC, American Foundrymen's Society, USA.

Fujiwara T. (2008). "Effect of aggregate on drying shrinkage of concrete." *Journal of Advanced Concrete Technology* 6(1), 31-44.

Goodhue M. J., T. B. Edil, et al. (2001). "Interaction of foundry sands with geosynthetics." *Journal of geotechnical and geoenvironmental engineering* 127(4), 353-362.

Guney Y., Y. D. Sari, et al. (2010). "Re-usage of waste foundry sand in high-strength concrete." *Waste Management* 30(8-9), 1705-1713.

Gurumoorthy N. and K. Arunachalam (2016). "Micro and mechanical behaviour of treated used foundry sand concrete." *Construction and Building Materials* 123, 184-190.

Ham R., W. Boyle, et al. (1986). "Comparison of leachate quality in foundry waste landfills to leach test abstracts." *Hazardous and Industrial Solid Waste Testing and Disposal: Sixth Volume*(933), 28.

Hooton R. (1993). "Influence of silica fume replacement of cement on physical properties and resistance to sulfate attack, freezing and thawing, and alkali-silica reactivity." *Materials Journal* 90(2), 143-151.

Jose J. and N. Hossiney (2016). "Characteristics of concrete containing waste foundry sand and slag sand." *Int J Earth Sci Eng* 9, 54-59.

Kaur G., R. Siddique, et al. (2012). "Properties of concrete containing fungal treated waste foundry sand." *Construction and Building Materials* 29, 82-87.

Khatib J., S. Baig, et al. (2010). Foundry sand utilisation in concrete production. *Second International Conference on Sustainable Construction Materials and Technologies, Citeseer*.

Khatib J., B. Herki, et al. (2013). "Capillarity of concrete incorporating waste foundry sand." *Construction and building materials* 47, 867-871.

Kleven J. R., T. B. Edil, et al. (2000). "Evaluation of excess foundry system sands for use as subbase material." *Transportation research record* 1714(1), 40-48.
Manoharan T., D. Laksmanan, et al. (2018). "Engineering properties of concrete with partial utilization of used foundry sand." *Waste Management* 71, 454-460.
Mast D. G. and P. J. Fox (1998). "Geotechnical performance of a highway embankment constructed using waste foundry sand." *Geotechnical Special Publication*(79), 66-85.
Mavroulidou M. and D. Lawrence (2019). "Can waste foundry sand fully replace structural concrete sand?" *Journal of Material Cycles and Waste Management* 21(3), 594-605.
Monosi S., F. Tittarelli, et al. (2013). "Effect of two different sources and washing treatment on the properties of UFS by-products for mortar and concrete production." *Construction and Building Materials* 44, 260-266.
Mushtaq S. M., R. Siddique, et al. (2021). "Experimental studies and drying shrinkage prediction model for concrete containing waste foundry sand." *Cleaner Engineering and Technology* 2, 100071.
NF EN 934-2 (2012). Adjuvants pour bétons, mortier et coulis - Partie 2 : adjuvants pour béton - Définitions, exigences, conformité, marquage et étiquetage.
NF EN 12350-2 (2019). Testing fresh concrete - Part 2: Slump test.
Parashar A., P. Aggarwal, et al. (2020). "Study on performance enhancement of self-compacting concrete incorporating waste foundry sand." *Construction and Building Materials* 251, 118875.
Prabhu G. G., J. H. Hyun, et al. (2014). "Effects of foundry sand as a fine aggregate in concrete production." *Construction and building materials* 70, 514-521.
Siddique R., G. De Schutter, et al. (2009). "Effect of used-foundry sand on the mechanical properties of concrete." *Construction and building materials* 23(2), 976-980.
Siddique R., G. Singh, et al. (2015). "Comparative investigation on the influence of spent foundry sand as partial replacement of fine aggregates on the properties of two grades of concrete." *Construction and Building Materials* 83, 216-222.
Singh G. and R. Siddique (2012). "Effect of waste foundry sand (WFS) as partial replacement of sand on the strength, ultrasonic pulse velocity and permeability of concrete." *Construction and Building Materials* 26(1), 416-422.
Thiruvenkitam M., S. Pandian, et al. (2020). "Use of waste foundry sand as a partial replacement to produce green concrete: Mechanical properties, durability attributes and its economical assessment." *Environmental Technology & Innovation* 19, 101022.
Torres A., L. Bartlett, et al. (2017). "Effect of foundry waste on the mechanical properties of Portland Cement Concrete." *Construction and Building Materials* 135, 674-681.
Vipulanandan C., Y. Weng, et al. (2000). Designing flowable grout mixes using foundry sand, clay and fly ash. *Advances in grouting and ground modification*, 215-233.
Zhu W., J. Wei, et al. (2016). "Understanding restraint effect of coarse aggregate on the drying shrinkage of self-compacting concrete." *Construction and building materials* 114, 458-463.

(2025); http://www.jmaterenvironsci.com